Structure of Tunnel Barrier Oxide for Pb-Alloy Josephson Junctions

The oxide formed on Pb-In and Pb-In-Au alloy films by processes similar to those used to fabricate oxide tunnel barriers for experimental Josephson junction devices has been investigated with transmission electron microscopy and diffraction (TEM/TED), Auger electron and x-ray photoelectron spectroscopies (AES and XPS), and ellipsometry. Thermal oxidation of Pb-In(13 at%) alloys at room temperature results in a noncrystalline oxide, whereas oxides formed at \geq 60°C in low pressures of O_2 result in a continuous stable epitaxial layer of cubic $In_2O_3\approx 2.5$ nm thick. The oxide formed by sputtering such a thermal oxide in an rf-excited O_2 glow discharge (rf oxidation) results in a layered structure \approx 6.5 nm thick, the bulk of which consists of an upper layer of epitaxial In_2O_3 and a lower layer of crystalline orthorhombic and tetragonal PbO. The thickness of the PbO layer depends on the availability of In at the metal-oxide interface, and thus, on the alloy composition and the temperature and rate of oxidation. For In concentrations above \approx 18 at%, the bulk of the oxide was found to be entirely epitaxial In_2O_3 . An additional \approx 0.3-nm-thick surface layer of PbO is observed, which arises from material sputtered from the Pb-coated rf electrode and subsequently backscattered onto the surface of the oxide. Altering this backscattered material from lead oxide to indium oxide increases the current densities of completed junctions by more than a factor of 40. In contrast, variations in the composition of the lower portions of the oxide have little effect on the junction characteristics. Factors affecting the composition and reproducibility of the oxide are discussed.

Introduction

Josephson junctions using Pb-alloy base electrode films containing In and Au as alloying constituents have been fabricated by several workers [1-5]. Junctions made with such alloys have shown an increased tolerance to repeated thermal cycling between room temperature and 4.2 K [3, 6, 7]. Since the tunnel barrier oxide is formed by oxidizing the base electrode, the presence of indium, the major alloying constituent, also affects the composition of the oxide. Although the tunneling characteristics of such junctions are acceptable for circuit fabrication, the possibility of having a mixed oxide in the tunnel barrier makes it difficult to characterize the properties of the tunnel barrier oxide and leads to the possibility that the oxide composition will be sensitive to details of the oxidation process. Previous studies of the thermal oxidation of Pb-In alloys have shown that a mixed oxide forms, with a strong preference for the formation of indium oxide [8, 9].

Ellipsometric measurements of oxides formed by rf oxidation have shown a strong dependence of the oxide index of refraction on alloy composition, indicating that a mixed oxide also forms as a result of rf oxidation [10]. In addition to being affected by the composition of the metal from which it is formed, the oxide composition can also be affected by the backscattering of material sputtered from the rf electrode on which the samples are mounted [11]. The material with which this electrode is coated has been found to have a strong effect on the current density of junctions [12].

Although the presence of a mixed oxide has been established, little has been known about the factors that influence its structure and composition. With the latter information, it should be possible to devise procedures by which the oxide composition may be made less sensitive

Copyright 1980 by International Business Machines Corporation. Copying is permitted without payment of royalty provided that (1) each reproduction is done without alteration and (2) the *Journal* reference and IBM copyright notice are included on the first page. The title and abstract may be used without further permission in computer-based and other information-service systems. Permission to republish other excerpts should be obtained from the Editor.

to process variables and more stable during subsequent storage and use. With these objectives in mind, we have studied the structure and composition of the oxides formed on Pb-In and Pb-In-Au alloy films under a variety of conditions. The structural information has come primarily from transmission electron microscopy (TEM) and diffraction (TED) studies, whereas the compositional information has come primarily from Auger electron spectroscopy (AES) studies. X-ray photoelectron spectroscopy (XPS or ESCA) studies have also provided valuable information regarding the oxide properties [11]. In this paper we describe the results of our studies of the properties of the oxides formed using processes similar to that described by Greiner et al. for fabricating experimental Josephson circuits [5]. We propose a model for the oxide and discuss the factors that determine the oxide structure and composition and their influence on some of the properties of the tunnel junctions. We also discuss several possible process modifications that may result in improved reproducibility of junction properties.

Experimental procedure

The procedure by which samples were prepared for the various investigations is described in this section. Variations in one or more steps of this procedure were sometimes required for a particular experiment and are noted where appropriate.

Samples were prepared in a vacuum chamber similar to that described by Greiner [13]. Films were deposited at room temperature from rf-induction-heated sources onto SiO_2 or SiO-coated Si wafers precleaned by sputter etching in O_2 . The films were deposited at pressures below 6×10^{-5} Pa by first evaporating 4.5 nm of Au at about 0.1 nm/s followed by Pb (\approx 3.5 nm/s) and In (\approx 0.5 nm/s) to give a total film thickness of 200 nm at the desired composition [14]. The films were then annealed in vacuum at room temperature for a minimum of 30 min to allow the layers to interdiffuse. As expected from consideration of the bulk diffusion coefficients [15], this period was sufficient for the components of the alloy to interdiffuse and for the films to approach their equilibrium structure.

Following the deposition and equilibration, the films were thermally oxidized by exposing them to a dynamic flow of O_2 at 2.7 Pa for 30 min at room temperature. The temperature was then increased to 75° C and the samples were oxidized in 2.7 Pa O_2 for 60 min. This two-step thermal oxidation process is referred to as 75° C thermal oxidation. If junctions were to be fabricated, the vacuum chamber was filled to atmospheric pressure with O_2 and the samples were removed for photoresist processing, in which the photoresist stencil for the counter electrode was applied. The rf oxidation was then carried out with

the samples mounted on a Pb-coated rf electrode capacitively coupled to a 13.56-MHz rf generator, which is used to excite a glow discharge in O₂. Energetic ions from the discharge bombard the samples [16], resulting in growth of an oxide film [1, 13, 17]. The rf oxidation was carried out in two stages, the first for 30 min at 10 Pa with 125 V (all voltages are peak-to-peak) applied to the electrode followed by an additional 30 min at 2.7 Pa and an rf voltage of 360 V [5]. If junctions were to be formed, this was immediately followed by deposition of a Pb-Au or Pb-Bi alloy counter electrode [5]. This four-step oxidation process, hereafter called the nominal rf-oxidation process, is similar to that which has been used in forming the tunnel barrier for experimental Josephson circuits [5].

Analysis of the oxide structure and composition by XPS and AES was carried out in most cases on samples exposed to room ambient for ≤30 min. Contamination of the sample was minor for short exposures. Samples were prepared for the TEM studies by depositing a total of 40 nm Pb plus In onto a photoresist or collodian film at a substrate temperature of 250 K. Typically, the rf oxidation was carried out immediately after the thermal oxidation. The films were then lifted from the substrate by soaking in acetone and floated onto a grid for mounting in the TEM instrument.

In some cases the progress of the oxidation was studied in a separate ultra-high-vacuum (uhv) system in which the films could be prepared using procedures similar to those described above and examined *in situ* with AES and ellipsometry [18]. The ellipsometer used a 632.8-nm-wavelength laser beam incident on the sample at 70° from normal. The oxide thickness was calculated from the measured ellipsometric parameters Δ and ψ using the FORTRAN program of McCracken [19].

Thermal oxide

• Oxidation at room temperature

Auger spectra were obtained from freshly deposited films within 5 min after deposition, and from these a Pb/In ratio characteristic of the bulk film composition was observed. On exposure of clean films to oxygen at 2.7 Pa, oxide grew to 1.0-1.3 nm within 1-2 min, after which little or no additional oxide grew. For \gtrsim 13 at% In, such oxides were found (AES) to consist almost entirely of indium oxide within the \approx 0.7-nm escape depth of the Auger electrons. An O/In peak-height ratio of 0.68 \pm 0.04, characteristic of In₂O₂, was consistently observed.

The results of an XPS experiment have further shown that the oxide consists almost entirely of In_2O_3 when it is formed at room temperature by gradual oxidation. A Pb-

In(13 at%) alloy was sputter-cleaned with Xe, resulting in the spectra shown in Fig. 1(a). The sample was then reoxidized by exposure to 1 Pa-s (10^4 langmuirs) of O_2 at 1×10^{-3} Pa followed by 30 min exposure at 2.7 Pa and 14 h at 10^5 Pa O_2 , resulting in the spectra shown in Fig. 1(b). The In 3d peaks have increased in intensity relative to the Pb 4f peaks and have shifted by 0.9 eV toward higher binding energies. The increase in intensity indicates that the oxide is predominantly oxidized indium, whereas the shift is characteristic of indium in In₂O₃ [11].

From these results, it is also possible to estimate the thickness L of this In₂O₂ layer. We note that the Pb peak has not shifted, indicating that it arises from electrons that are excited in the underlying metal and escape through the overlying oxide layer. This is confirmed by the spectra shown in Fig. 1(c), in which the sample has been tilted such that the angle θ between the photoelectron detector and the sample surface was decreased. This results in a decreased escape depth normal to the surface [11, 20] and thus enhances the signal from the material nearest the surface. By analyzing the change in ratio of the intensity of the In peak to that of the Pb peak from the metal using the method discussed in Ref. [11], we find for the oxide thickness $L = 1.3\lambda = 2.3 \pm 0.3$ nm, assuming $\lambda = 1.74$ nm for the escape depth of Pb 4f electrons in In₂O₃. This is in good agreement with ellipsometrically determined thicknesses for Pb-In alloy films oxidized at atmospheric pressure [9].

A small shoulder is also visible on the low-energy side of the Pb 4f peaks, suggesting that some lead oxide may be present. The increase in the intensity of the shoulder relative to that of the peak originating in the metal at smaller θ also shows that the shoulder arises from Pb in the oxide layer. It is interesting to note that the chemical shift of the oxidized Pb is 1.8 eV, considerably greater than the ≤ 1 eV from known oxides of Pb (see sources cited in Ref. [11]). This suggests that the lead oxide is not present in the form of isolated particles, but rather is mixed on an atomic scale with the indium oxide [11].

The TEM studies were carried out on Pb-In alloy films containing 11.4, 15.2, and 23.8 at% In, which were oxidized at room temperature in \approx 2 Pa $\rm O_2$ and in air during transfer of the samples to the electron microscope. However, none of the films showed evidence of a crystalline oxide layer, either in the micrograph or the diffraction pattern. It is likely that the thermal oxide formed at room temperature was not sufficiently ordered to be detected by TEM.

The fact that the oxide grown on Pb-rich alloys is predominantly In₂O₃ is a consequence of the lower free en-

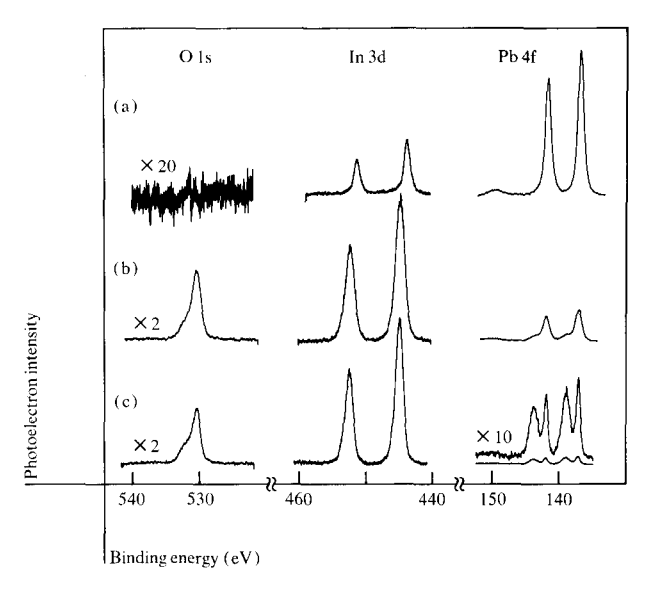


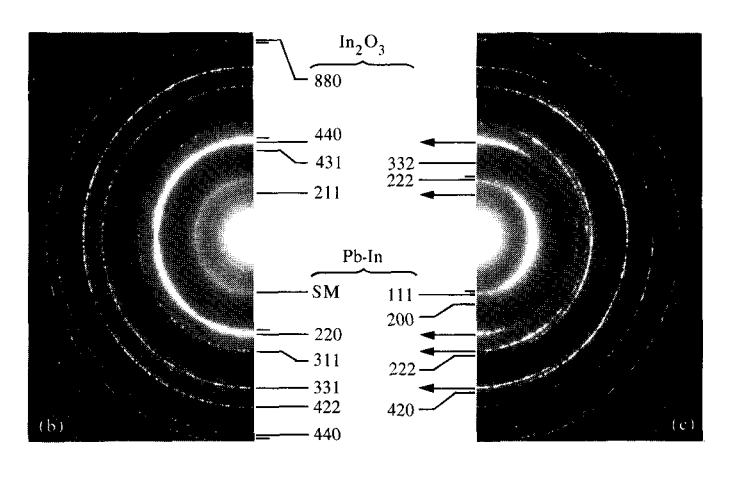
Figure 1 X-ray photoelectron spectra from a Pb-In(13 at%) alloy film using Al K α x-rays; (a) sputter-etch-cleaned film taken at a detection angle $\theta = 65^{\circ}$ from glancing; (b) after oxidation at 10^{-3} , 2.7, and 10^{5} Pa for a total exposure of 5×10^{9} Pa-s, same θ ; (c) as in (b) except $\theta = 28^{\circ}$.

ergy of In₂O₃ compared to PbO. If the system were in thermodynamic equilibrium, only trace amounts of PbO would be present in the oxide [8]. The formation of any PbO must therefore be a result only of kinetic limitations in the rate at which In can be supplied to the oxide-metal interface from the Pb-rich film. A consequence of this behavior is that the oxide composition is sensitive to the oxide growth rate. This sensitivity is evident in comparing our results with those of Chou et al. [8]. They observed about four times more PbO at the surface of a Pb-In(13 at%) alloy oxidized by "immediate" exposure to O₂ at atmospheric pressure, a procedure which results in a more rapid oxide growth rate. Since kinetic factors appear to be important in determining the oxide composition, temperature would also be expected to be a factor in determining the oxide composition.

• Oxidation at elevated temperatures

In the course of preparing oxides by rf oxidation at elevated temperatures, one sample was thermally oxidized at room temperature and 2.7 Pa followed by thermal oxidation at 60° C at pressures ranging between 0.7 and 10 Pa for ≈ 2 h. Studies of this sample by TEM and TED showed that crystalline In_2O_3 had formed, as indicated in Fig. 2. In the diffraction pattern shown in Fig. 2(b), rings from the $\{211\}$, $\{440\}$, and $\{222\}$ reflections of cubic In_2O_3 are visible. In addition, the In_2O_3 has a definite orientation with respect to the alloy, as indicated by the correlation of the intensity modulation along the diffraction rings





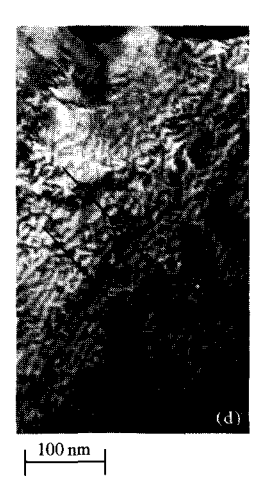


Figure 2 TED patterns and micrographs from an \approx 40-nm-thick Pb-In(12.4 at%) film oxidized at 60°C in \approx 3 Pa O₂ for \approx 100 min. Parts (a) and (b) were taken with the 75-keV beam normally incident on the film, whereas the film was tilted for (c) and (d) such that the dark-field image is formed from the {111} reflections of Pb-In. Arrows refer to features labeled in the opposing pattern; the short lines indicate the second ring of a closely spaced pair, this ring being labeled in the alternate half of the same pattern. The Pb-In ring labeled SM is a subsidiary maximum or satellite peak related to the metal film. The marks shown in (a) and (d) were used in determining the fringe spacing.

Table 1 Measured and calculated spacing of Moiré fringes between cubic In₂O₃ and Pb-In alloy.

Sample 12.4 at% In; 60°C thermal oxidation	Interplanar spacing (nm)				Moiré fringe spacing (nm)	
		bIn	I	n_2O_3	Calculated	Measured
	{220} {111}	0.1742; 0.2844	{440} {222}	0.1788; 0.2921	6.8 10.8	7.1 ± 0.6 11.2 ± 1.0
25 at% In, rf oxidation	{220} {111}	0.1733; 0.2830	{440} {222}	0.1788; 0.2921	5.6 9.0	5.3 8.2

of Pb-In and In_2O_3 . The orientational relationship of the diffracted beams can be seen quite clearly from diffraction patterns from single grains on which an rf oxide has been grown (shown later) from which it is evident that the cubic In_2O_3 has grown *epitaxially* on the individual grains of the face-centered-cubic alloy film.

The high degree of epitaxy of the In_2O_3 is also evident in the micrographs from this sample, as shown in Figs. 2(a) and (d), in which striking Moiré fringes are seen. The Moiré fringes seen in the bright-field micrograph [Fig. 2(a)] arise from the interference between electrons scattered from the {220} planes of the alloy and the {440} planes of the In_2O_3 . The difference in spacing of the (440) plane of In_2O_3 and the (220) plane of Pb-In is such that they are coincident every 39 planes, corresponding to a fringe spacing of 6.8 nm. If the average fringe spacing is measured, as shown in Fig. 2(a), a value of 7.1 ± 0.6 nm is found, in excellent agreement with the calculated value

(Table 1). Similar results are obtained from diffraction patterns and dark-field micrographs obtained from this sample in a tilted configuration. The {111} ring from Pb-In and the {222} ring from In₂O₃ are clearly visible in the diffraction pattern from a tilted sample [Fig. 2(c)]. Figure 2(d) shows the dark-field micrograph obtained from this pair of reflections. Again, Moiré fringes arising from interference between these two planes are quite apparent and, as shown in Table 1, the observed and calculated fringe spacings are in good agreement. Thus, in contrast to the oxide grown at 24°C, the oxide grown at 60°C is highly ordered and in almost perfect epitaxy with the alloy. It also appears from the micrographs that the In₂O₂ is continuous and in registry with the alloy over an entire grain of alloy with no evidence of dislocations or grain boundaries within the oxide layer.

Auger spectra suggest that the primary effect of the high-temperature oxidation is to form crystalline In₂O₃, as

observed with TEM, rather than to cause a change in the composition of the oxide. When a sample oxidized at room temperature and 2.7 Pa was further oxidized at 75 $^{\circ}$ C and 2.7 Pa, no change was observed in the Auger spectrum. From these results we also draw the conclusion that the observed O/In ratio of 0.68 is characteristic of In₂O₃.

As mentioned previously, oxidation at 24°C and 2.7 Pa essentially ceases after about 1.3 nm of oxide has formed. However, when the temperature is increased to 75°C the film begins to grow again, with the thickness increasing approximately logarithmically with time, as determined ellipsometrically. This leads to a film thickness of $\approx 2.5-3.0$ nm after 60 min of oxidation. One such film was subsequently exposed to oxygen at 10^{5} Pa for 16 h at 24°C , in which case the thickness increased by about 0.4 nm, a portion of which could have been due to adsorbed O_{2} molecules. Thus the increased thickness obtained at high temperature appears to have resulted in a negligible growth rate at 24°C , even at greatly increased pressures.

• Oxide stability

The epitaxial In₂O₃ formed as a result of the 75°C thermal oxidation has also been found to remain effectively unchanged when exposed to atmosphere and the chemical ambients typically used for Josephson circuit fabrication [5]. A sample on which such an oxide had been grown and characterized was processed through all steps used for preparing a typical photoresist stencil [21]. The sample was then returned to the uhv system for analysis. The measured thickness change was less than 0.3 nm (comparable to the experimental reproducibility) and the O/In ratio as observed with AES changed by less than 3%. Additionally, there was no evidence for carbon contamination of the surface of this particular sample.

By contrast, photoresist processing was found to produce significant changes in the composition of the mixed PbO/In₂O₃ oxide that forms on a Pb-In(13 at%) film when exposed directly to O, at atmospheric pressure. The processing reduced the amount of lead oxide by about a factor of three. This composition change was found to occur during the basic aqueous developing and rinsing steps, which is reasonable in view of the solubility of PbO in H₂O and alkaline solution [22]. In addition, the thickness of an oxide grown at room temperature is still sufficiently small that it would continue to grow in air. To the extent that the growth rate of such an oxide depends on the ambient conditions, including processing in aqueous solution, the final thickness can be dependent on variations in these conditions. As will be shown, the composition of the completed tunneling oxide can be affected by the nature of the initial thermal oxide. Thus, the greater stability of the initial oxide grown using the 75°C oxidation process

should result in the formation of more reproducible tunneling oxides. Based on these findings, the 75°C thermal oxidation process has been incorporated into the tunnel barrier formation process used to fabricate exploratory Josephson integrated circuits [5].

RF oxide

The rf oxidation process is characterized by a very rapid initial growth that decreases in an exponential manner with increasing oxide thickness [1, 10, 13, 17]. The growth kinetics have also been found to depend on the pressure and rf voltage conditions during oxidation [13, 17]. Since the composition of the thermal oxide formed on Pb-In alloy films was found to depend on the growth kinetics, we would expect the composition of the oxide formed on such films by rf oxidation also to be dependent on the rf-oxidation conditions.

The effect of the first step of the rf-oxidation sequence has been studied on samples that were thermally oxidized at 75°C and then transferred to the uhv system after exposure to air or photoresist processing. Auger spectra obtained in situ after this pre-clean step [10 Pa O_2 at 125 V for 30 min] have shown that any carbon initially present was removed and that the oxide surface was In_2O_3 . The thickness of the oxide was found to increase by ≈ 1 nm as a result of this process. Thus, this step of the rf-oxidation process is effective in removing contaminants that may be present as a result of photoresist processing, resulting in a more reproducible oxide at the start of the next step of the oxidation process.

The second and primary step of the rf-oxidation sequence consists of sputtering the sample at room temperature, typically for 30 min in 2.7 Pa of oxygen at an rf voltage of 360 V. We now describe TEM, XPS, AES, and ellipsometry studies of oxides formed under such conditions. The effects of alloy concentration, temperature, and starting oxide on the final oxide structure are also explored.

◆ Oxide structure—TEM/TED

We first describe the TEM analysis of an oxide formed by the nominal rf-oxidation process on a Pb-In(12.5 at%) alloy. Diffraction patterns from this sample show the presence of In₂O₃ and both the orthorhombic and tetragonal modifications of PbO. Bright- and dark-field micrographs of the same region of this sample are given in Figs. 3(a) and (b), respectively, and show the presence of all three oxides. The Moiré fringes between In₂O₃ and the Pb-In alloy are most evident in the dark-field micrograph, but can also be readily detected in the bright-field micrograph. Thus the presence of an epitaxial layer of In₂O₃ is evident, as was the case for the oxide formed thermally at

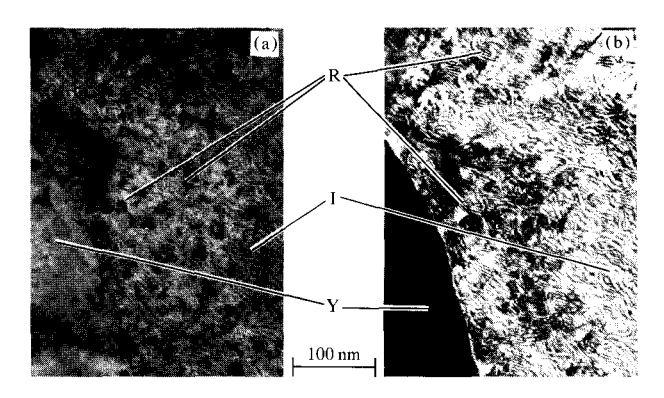


Figure 3 Bright-field (a) and dark-field (b) micrographs from the same region of a Pb-In(12.5 at%) alloy that had been rf oxidized using the nominal process. The Moiré fringes are the same as described in Fig. 2; labels are described in the text.

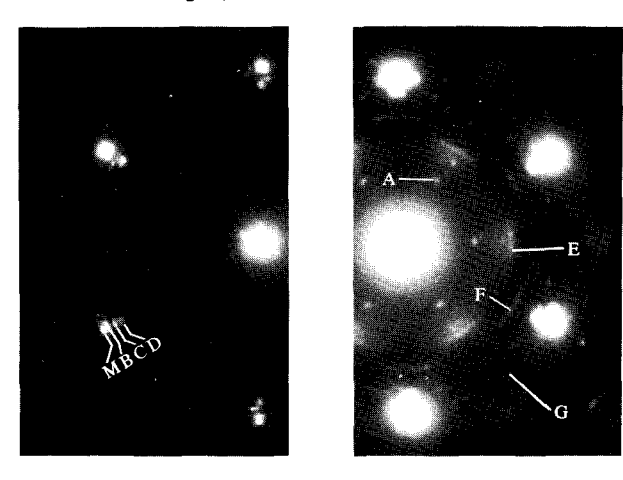


Figure 4 Diffraction pattern from a single grain of the same sample in Fig. 3, showing the orientational relationship of the oxides. The diffraction spots are: Pb-In—M {220}; In₂O₃—A {211}, B {440}; tetragonal PbO—C {112}, D {200}; orthorhombic PbO—E (200), F (020), G (220).

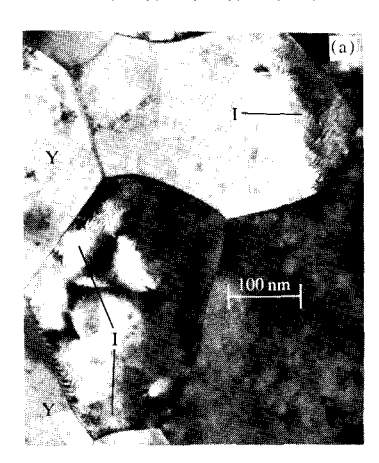




Figure 5 Bright-field (a) and dark-field (b) micrographs of a Pb-In(11.4 at%) film that was thermally oxidized at room temperature followed by rf oxidation at 2.7 Pa, 360 V at 24° C for 30 min. Islands of tetragonal PbO are labeled R; the texture on the grains labeled Y is characteristic of orthorhombic PbO. Moiré fringes due to In_2O_3 , labeled I, are visible in the vicinity of the grain boundaries in (a).

high temperature; but it is not clear whether this is the original thermally grown oxide, or whether the original oxide has been removed by sputtering and additional In_oO_o (designated I) has been grown. This question will be addressed later. A large number of individual grains of red, tetragonal lead oxide (designated R) are visible in both micrographs as high-contrast Moiré fringes. Similar grains of red PbO have been observed in oxides grown on Pb by Matthews et al. and they have discussed the properties of these epitaxial grains in detail [23]. The grains seen in Fig. 3, however, appear to be considerably smaller than those seen on Pb. Lastly, an essentially continuous layer of yellow, orthorhombic PbO appears to cover the surface. This is most evident in the grain at the lower left of Fig. 3(a), in which a mottled texture (designated Y) is apparent across the whole grain. This is very similar to the yellow PbO seen on Pb [24]. The apparently continuous nature of the yellow PbO and the In₂O₂ suggests that they are present as layers, one above the other.

Although it is clear from the Moiré fringes that the red PbO and the In₂O₃ are epitaxial on the Pb-In, the orientation of the yellow PbO is not evident. To resolve this question, diffraction patterns were obtained from single grains of the alloy. Two such patterns are shown in Fig. 4. The spots labeled A and B arise from reflections from the {211} and {440} planes of cubic In₂O₂. The sharpness of these spots and their orientation relative to the Pb-In (M) spots show conclusively that the In₂O₃ grows with a very high degree of epitaxy on the Pb-In. The spots labeled C and D arise from the (112) and (200) reflections of tetragonal PbO. These are almost identical to those observed in the diffraction pattern from oxidized Pb, and are discussed in detail by Matthews et al. [23]. Orthorhombic PbO is evidenced by the arcs labeled E, F, and G, corresponding to the (200), (020), and (220) reflections, respectively. These also are nearly identical to those observed from oxidized Pb and, as discussed by Matthews et al. [24], show that the orthorhombic PbO grows on the lead alloy with a preferred orientation. The fact that the two modifications of PbO grow in an oriented manner suggests that the PbO has grown at the oxide-metal interface underneath the layer of In₂O₃. This hypothesis is confirmed by the results of the XPS study [11], as will be discussed in detail later.

Effect of In concentration The effect of In concentration in the alloy on the composition of the rf oxide was examined for samples that were thermally oxidized at 24°C for 30 min in 2.7 Pa O₂ and then rf oxidized in 2.7 Pa O₂ at 360 V and 24°C for 30 min. Table 2 summarizes the composition of the oxide as determined from TEM/TED observations for alloys of varying In concentrations. For an In concentration of 9 at% very little crystalline In₂O₃

Table 2 Composition of oxides grown by rf oxidation of Pb-In alloys of different compositions as determined by TEM/TED*.

In concentration (at%)	P	$Cubic\ In_2O_3$		
	orthorhombic	tetragonal		
9	Yes	Yes	Trace in real image, not detectable in diffraction Visible in real image, faintly in diffraction pattern	
11.8, 11.4	Yes	Yes		
14.4	Yes	Yes	Yes—epitaxial	
17.1	Very little	Yes	Yes—epitaxial	
18.2	Not detected	Not detected	Yes—epitaxial	
25.5	Not detected	Not detected	Yes—epitaxial	
100	No	No	Yes—epitaxial	

^{*}Oxides were formed by thermal oxidation in 2.7 Pa O, at 24°C and subsequent rf oxidation in 2.7 Pa O,, rf voltage = 360 V, 24°C for 30 min.

was detected in the oxide. The only indication of In₂O₂ was found in small regions near the grain boundaries where several Moiré fringes like those shown in Figs. 2 and 3 can be seen. As seen in Fig. 5, at an In concentration of 11-12 at%, In₂O₃ is apparent near the grain boundaries (regions labeled I) but is not visible in the center regions of the grains. Very faint features attributable to In₂O₃ are visible in the diffraction patterns from these samples. The sample containing 14.4% In showed definite diffraction spots from the {211} and {440} planes of In₉O₃, but in this case the diffraction features from orthorhombic PbO were weak. Moiré fringes from In₂O₃ were visible over most of the grain, but again were stronger in the vicinity of the grain boundaries. When the In concentration was increased to 17%, the oxide became almost entirely In₂O₂. Moiré fringes covered an entire grain and In₂O₃ reflections were quite evident in the diffraction patterns. Only very weak spots or rings from either form of PbO were visible in the diffraction patterns and only relatively few small islands of red PbO were seen in the micrographs.

For In concentrations above 18% only In₂O₃ was seen with TEM or TED; no evidence was found for either of the modifications of PbO. At these concentrations each Pb-In grain was covered with an epitaxial layer of cubic In₂O₃, resulting in Moiré fringes similar to those shown in Fig. 2 for the 75°C thermal oxide. The higher In concentration in the alloy has decreased the Pb-In lattice constant slightly [25], so the spacing of the Moiré fringes between In₂O₃ and Pb-In has decreased, as shown in Table 1. These results demonstrate that the composition and structure of the rf oxide can be strongly influenced by the alloy concentration, in agreement with previous studies

that used AES or ellipsometry and concluded that for both thermal and rf oxidation only In_2O_3 is grown for In concentrations above 25 at% [8-10].

These results suggest a picture in which In₂O₃ forms initially, depleting the surface region of the alloy of In and leaving only Pb available to combine with the oxygen. Thus, the amount of In₂O₃ formed would depend on the amount of In within some effective diffusion distance of the surface, this amount depending directly on the In concentration of the alloy. However, due to the rapid decrease in the rate of oxidation with increasing oxide thickness, the amount of In2O3 formed may be a supralinear function of the In concentration. As the growth rate slows, the effective diffusion distance should increase. Thus, above some concentration, the In that has combined with the oxygen may be resupplied by diffusion from the bulk. Interesting evidence for this hypothesis is provided by the electron micrographs for the 11-12 at% In alloys in which, as noted earlier in connection with Fig. 5, the In₂O₃ is seen to form preferentially at grain boundaries. A possible explanation for this phenomenon is that even though the In has been depleted in the center of the grain, the region near the boundary continues to be supplied with In as a result of the relatively rapid diffusion of In within the grain boundary region.

Effect of temperature TEM observations of a sample rf oxidized at 60° C have shown more In_2O_3 than observed on a sample similarly oxidized at 24° C (the sample of Figs. 3-4). When the diffraction patterns of the 24° C and 60° C oxides are compared, the {211} and {440} rings from In_2O_3 for the latter are found to be significantly more intense relative to those of the alloy. The higher level of

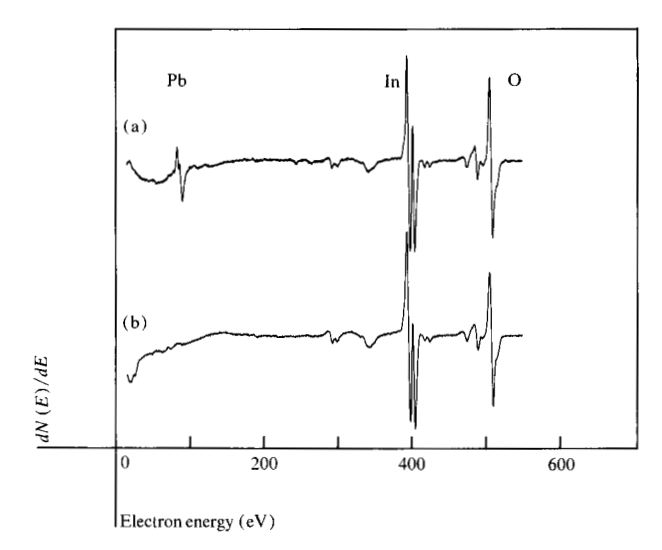


Figure 6 Auger spectra from Pb-In films on which the oxide was grown using the nominal rf-oxidation process; (a) 10.6 at% In alloy on Pb-coated rf electrode, (b) 13.5 at% In alloy on Incoated rf electrode.

 In_2O_3 in the 60°C oxide is not evident from the micrographs, however. The texture of the 60°C oxide appears to be much finer than for the 24°C oxide. Although Moiré fringes can be seen, they are either obscured by the finer grain size of the PbO or the In_2O_3 may itself be contributing to the finer grain size. In either case, it is clear that the concentration of crystalline In_2O_3 is increased by oxidation at high temperature, in accord with the hypothesis that the amount of In_2O_3 formed is dependent on the rate at which In can be supplied from the underlying Pb-In film.

Effect of initial oxide Films that were thermally oxidized under different conditions but rf oxidized under the same conditions were also analyzed. The micrographs for the sample oxidized using a 60°C thermal oxidation process prior to rf oxidation (Fig. 3) indicate an In_2O_3 layer over the entire surface. However, when the thermal oxide was grown at room temperature [Fig. 5(a)], In_2O_3 is visible only in small quantities near the grain boundaries. The diffraction patterns from these samples also indicate that the 60°C sample contains significantly more In_2O_3 . These results indicate that the oxide formed prior to rf oxidation is important in determining the properties of the final oxide and they suggest that a considerable portion of the original thermal oxide remains after the rf oxidation.

Oxide structure—XPS/AES

Backscattered material Thus far we have considered only factors that influence the composition of the oxide grown from the Pb-In alloy film. In a glow-discharge envi-

ronment, however, material sputtered from the surface of the electrode surrounding the sample can be backscattered from the gas molecules onto the sample surface [26]. Evidence for backscattering during rf oxidation can be seen in Fig. 6, which shows Auger spectra for samples oxidized on rf electrodes coated with Pb [Fig. 6(a)] and In [Fig. 6(b)], all other conditions being nominally identical.

The influence of backscattering on the composition of rf oxides has been investigated using XPS [11]. Samples of Pb-In(12 at%), Pb-In(25 at%), and pure In were examined after the nominal rf-oxidation process. The XPS spectra were all nearly identical. In particular, the ratio of the intensities of the Pb 4f to the In 3d peaks was essentially independent of the sample composition, indicating that the observed Pb did not originate from Pb in the alloy. A detailed analysis of data obtained using a variable detection angle method has indicated that the equivalent of ≈ 0.3 nm of lead oxide is concentrated at the surface of a "thick" layer of indium oxide [11]. Thus, the surface composition of an rf oxide can be affected by the backscattering of material sputtered from the rf electrode. No evidence was found for backscattered lead oxide using TEM, probably because it was too thin to be detected.

The amount of backscattered material has also been found to depend on the rf-oxidation conditions. One of the samples studied with XPS, oxidized at 6.7 Pa for 120 min, was found to have about twice as much lead oxide at its surface as samples oxidized at 2.7 Pa for 30 min [11]. This result can be attributed to an increased backscattering rate from the higher density of oxygen molecules. Studies currently in progress [18] have confirmed this dependence on oxygen pressure. In addition, it has been found that the rate at which the backscattered Pb accumulates on the surface of the oxide depends strongly on the sputtering voltage. This is due to the increased sputter-etch rate at higher voltages. Thus, through backscattering, the surface composition of the oxide can be affected by the pressure, the rf voltage, and the oxidation time. As will be discussed, the current density of Josephson junctions in which the tunneling oxide was formed by the combined use of thermal and rf oxidation was found to be strongly influenced by backscattering during the rf oxidation portion of the process.

Bulk oxide structure The XPS analysis of the oxide formed using the nominal rf-oxidation process also provides information about the "bulk" of the oxide. As noted previously, a "thick" layer of In_2O_3 was observed below the backscattered lead oxide on the Pb-In(12 at%) alloy. However, TEM analysis of a similar sample showed crystalline layers of both In_2O_3 and PbO (cf. Fig. 3). This PbO layer must therefore lie between the In_2O_3

Table 3 Measured ellipsometric parameters from rf oxides on Pb-In alloys with calculated values for oxide thickness and refractive index1

Sample	Δ	ψ	$n_{ox}(n_s)$	$\kappa_{ox}(\kappa_s)$	L (nm)
Pb-In(34 at%)					
Clean film	129.00	35.35	(2.14)	(2.14)	_
Thermal oxide	124.48	35.51	1.9	0.05	2.5
RF oxide ³	118.81	35.56	1.9	0.09	5.7
			2.68	0	4.2
Pb-In(12 at%)					
Clean film	127.34	34.45	(2.18)	(1.99)	_
Thermal oxide	122.00	34.06	1.9	0.55	2.8
RF oxide	112.98	34.16	2.35	0.20	7.0
			2.8	0.14	6.0
$\Delta L_{ m rf}^4$			2.8	0.03	3.7
$L_{\rm thermal}^{\rm rr} + \Delta L_{\rm rf}$					6.5

^{&#}x27;Thermal oxides were grown in 2.7 Pa O_a, 30 min at 24°C and 60 min at 75°C; rf oxides were additionally oxidized in 2.7 Pa O_a, 360 V, 24°C for 30 min on a Pb-coated rf electrode

layer and the alloy. Since this PbO layer does not contribute significantly to the intensity of the Pb 4f peak from the oxide, the thickness of the In₂O₃ layer must exceed the escape depth of ≈ 1.7 nm for Pb 4f photoelectrons [11]. The similarity in thickness of this In₂O₃ layer and the initial thermal oxide suggests that the thermal oxide has remained essentially intact throughout the rf-oxidation process. This interpretation is consistent with measurements of the rate (0.01-0.04 nm/min) [18, 27] at which In₂O₃ is sputtered away as a result of bombardment with oxygen ions from the rf plasma under these conditions (360 V, 2.7 Pa).

• Oxide thickness

Because the rf oxide is in general a mixture of three oxides, an accurate determination of the total oxide thickness is quite difficult. The situation is further complicated because In₂O₃ is generally highly conducting and thus has a non-negligible imaginary contribution κ to its index of refraction $n^* = n(1 - i\kappa)$. This makes a unique determination of the oxide thickness by standard ellipsometry impossible, even for a single component oxide [28]. However, the oxide thickness can be calculated if a value for nor κ is assumed [28]. Since the oxides formed on alloys with high In concentration were found to be entirely In_2O_3 , we have used n = 1.9, the value reported for bulk In_nO_n [29]. For this fixed value of n, values of oxide thickness and extinction coefficient κ were calculated from the ellipsometric measurements, as shown in Table 3. For a Pb-In(34 at%) alloy, thicknesses of 2.5 and 5.7 nm were obtained for the thermal and rf oxides, respectively. Our choice of n = 1.9 resulted in calculated κ values of ≈ 0.07 , which are reasonable because In, O3 is known to be a conducting, oxygen-deficient semiconductor [29], and high carrier levels would be expected to lead to optical absorption. If we assume $\kappa = 0$, we calculate a thickness L =4.2 nm and n = 2.68, an unreasonably large value [29]. Donaldson and Faghihi-Neiad used the assumption that $\kappa = 0$ to interpret their ellipsometric measurements for rfoxidized Pb-In alloys. For high In concentrations they reported $L \approx 4$ nm and n = 1.9 [10]. We would expect their oxides to be similar to ours and cannot account for the disparity in the results.

For the case of a Pb-In(12 at%) alloy the determination of the thickness of an rf oxide becomes more complicated, since both PbO and In₂O₂ layers are present. We have estimated the thickness for this case two ways: In the first, it was assumed that the oxide consists of equal amounts of PbO and In_0O_0 and that n is the average of the n values for the individual oxides, resulting in a calculated thickness of 7 nm. (For comparison, the 6-nm value obtained assuming n = 2.8, the value for PbO, is also shown in Table 3.) In the second, the substrate is taken to be the metal plus the thermal oxide and we have calculated the thickness increase $\Delta L_{\rm rf}$ assuming that only PbO forms as a result of the rf oxidation. This procedure results in a total thickness of 6.5 nm, in reasonable agreement with the result of the first method.

An estimate of the thickness of the rf oxide formed on a Pb-In(12 at%) alloy can also be obtained from the slight shoulder evident in the Pb peaks of the XPS spectrum shown in Fig. 7. When each peak is resolved into two components, it is seen that the shoulder is due to a small narrow peak ≈1.1 eV from the main peak. Although this

⁽nominal process).
²Measured with $\lambda = 632.8$ nm light, 70° angle of incidence; Δ_0 , ψ_0 measured on clean metal film.
³RF voltage was slowly increased to 360 V, oxidized for a total of 160 min.

Substrate assumed to be thermal oxide.

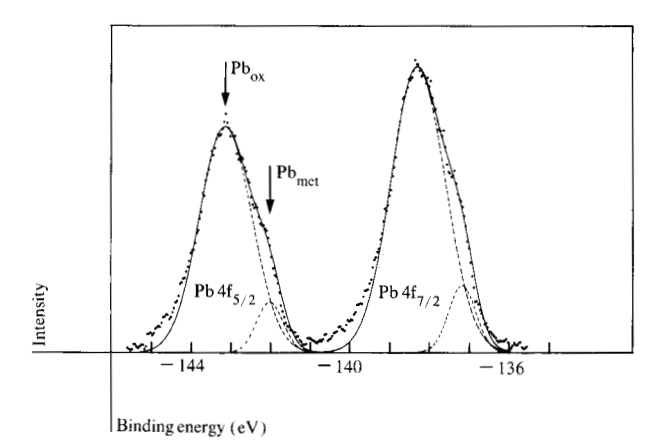
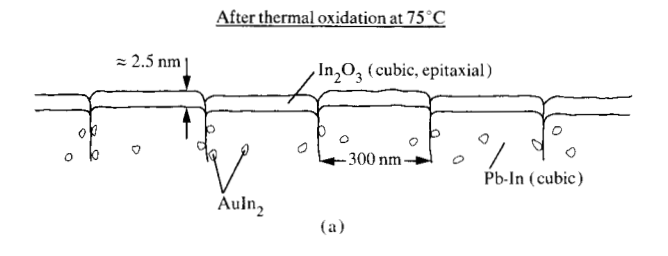


Figure 7 XPS spectrum of the Pb 4f levels taken at $\theta=65^\circ$ from glancing from a Pb-In(13 at%) alloy on which the oxide was formed using the nominal process on a Pb-coated rf electrode. Each peak is resolved into two Gaussian components (---), corresponding to Pb in the oxidized state at the surface of the oxide and Pb in the metallic state in the alloy beneath the oxide.



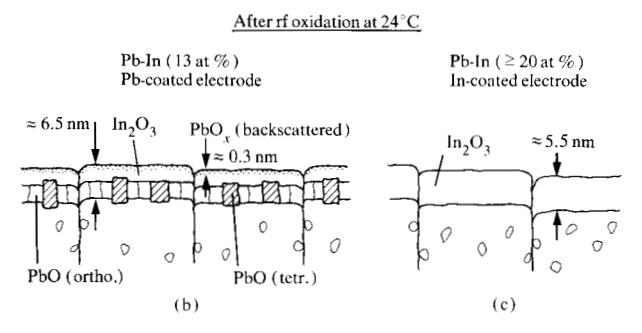


Figure 8 Schematic illustration of the oxide structure resulting from several different oxidation procedures. (a) In_2O_3 layer after thermal oxidation at $\approx 75^{\circ}\text{C}$, 1–10 Pa O_2 ; (b) ≈ 13 at% In alloy with thermal oxide as in (a) after nominal process; (c) oxide resulting from rf oxidation of a ≈ 20 at% In alloy on an In-coated rf electrode.

small peak is ≈ 0.3 eV below the predicted position of the metal peak, its width suggests that it arises from metallic Pb in the alloy. If we assume that the main peak arises primarily from the 0.3 nm of lead oxide at the surface and that the small peak is due to electrons from the metal which have been attenuated by the oxide, we calculate a

total oxide thickness of \approx 6 nm, in good agreement with the values determined ellipsometrically.

Summary of oxide structure

It is seen from the results presented that the rf-oxide structure and composition are affected by the alloy composition and by both the thermal and rf-oxidation conditions. In general, the three oxide phases (the orthorhombic and tetragonal forms of PbO and cubic In₂O₃) are formed in a complex mixture. In certain cases, however, simpler structures can be obtained. For example, thermal oxidation of a Pb-In(13 at%) alloy at 75°C and 2.7 Pa forms an epitaxial layer of $In_2O_3 \approx 2.5$ nm thick [see Fig. 8(a)]. Subsequent rf oxidation of such a sample (nominal rf-oxidation process) results in a layered structure \approx 6.5 nm thick [Fig. 8(b)]. A PbO layer of about half the total thickness has grown between the epitaxial In₂O₃ and the metal alloy. In addition, about a monolayer (≈ 0.3 nm) of oxide has been deposited on the surface as a result of backscattering of Pb sputtered from the Pb-coated rf electrode on which the samples were mounted. Figure 8(b) illustrates the case for a sample prepared on a Pb-coated electrode. Even simpler rf-oxide structures were obtained when alloys of In concentration ≥20 at% were used. In these cases, only epitaxial In₂O₃ was observed; i.e., the underlying layer of PbO was eliminated. When such samples were rf oxidized on an In-coated rf electrode the layer of backscattered lead oxide was also eliminated, and the structure shown in Fig. 8(c) was obtained.

Tunnel current density

The ability to prepare oxides with and without the underlying PbO and/or the layer of backscattered Pb has enabled us to explore the effects of these layers on the current density of junctions. The effect of the lower PbO layer was tested by making junctions on 13 and 22 at% In alloys using the nominal rf-oxidation process and a Pbcoated rf electrode. The oxide structure for the 13 at% alloy should be similar to that shown in Fig. 8(b), while that for the 22 at% alloy should be like the oxide shown in Fig. 8(c) with the addition of a backscattered lead oxide layer. The measured current-voltage (I-V) curves for junctions prepared with Pb-Bi(28 at%) counter electrodes are shown in Fig. 9 (Curves 1 and 2). It can be seen that the current density for both alloy compositions is almost the same. Another experiment using an In-coated electrode has shown less than a factor of two difference in current density between two samples with In concentrations of 13 and 27 at% [30]. This surprising result indicates that the current density depends only weakly on the composition of the lower "half" of the oxide.

The effect of the backscattered material on the junction current density was tested by making junctions on Pb-

In(22 at%) base electrodes using the nominal rf-oxidation process. One group of junctions was prepared on a Pbcoated rf electrode, another on an In-coated electrode. The junction counter electrode used for both of these was a Pb-Au(1.8 at%) alloy. The I-V characteristics for these junctions are shown as Curves 3 and 4 in Fig. 9 [31]. The current density of the junctions prepared on the In-coated electrode (Curve 4) are higher by a factor of ≈40 than those prepared on the Pb-coated electrode (Curve 3). This effect was first observed by Greiner and Basavaiah [12], who found an increase in current density of $\approx 10^3$ for junctions prepared on In-coated electrodes compared with that for junctions prepared on Pb-coated electrodes. Such current densities are higher than those which have been used for Josephson integrated circuits [32]. At present, we do not have an adequate explanation for the strong effect that the backscattered material has on the current density of completed junctions. One possibility is that the surface composition of the oxide affects the barrier height at the oxide-counter electrode interface. Another possibility is that the surface composition may affect the thickness of the tunneling oxide by altering the growth kinetics of the oxide, e.g., by changing the surface concentration of oxygen and/or the potential across the growing oxide [17]. In any event, in contrast to the lack of sensitivity of the tunnel current density to the composition of the lower 2-3 nm of the oxide, it is clear that the nature of the approximate monolayer of backscattered material on the upper surface of the tunneling oxide has a very marked effect on the current density.

Conclusions

We have found that oxides prepared by thermal oxidation followed by rf oxidation of Pb-In and Pb-In-Au alloy films consist in general of a mixture of PbO and In₂O₃, with a thin layer of backscattered material at their surface. Under certain oxidation conditions simpler structures can be formed. Variations in the surface composition of the oxide produced by varying the material backscattered during rf oxidation from lead oxide to In₂O₃ had a strong effect on the current density of completed tunnel junctions. By contrast, variations in the composition of the portion of the oxide adjacent to the base electrode produced by varying the In concentration in the base electrode had little effect on the junction characteristics.

The results presented here suggest several ways in which the composition and structure of the tunnel barrier oxide might be made more reproducible and stable. The thermal oxidation of the base electrode films at 24 and 75°C in 2.7 Pa $\rm O_2$ prior to removal from the vacuum system produces an epitaxial $\rm In_2O_3$ oxide layer, which is more stable during subsequent processing. By utilizing an alloy containing In concentrations exceeding ≈ 20 at%, or

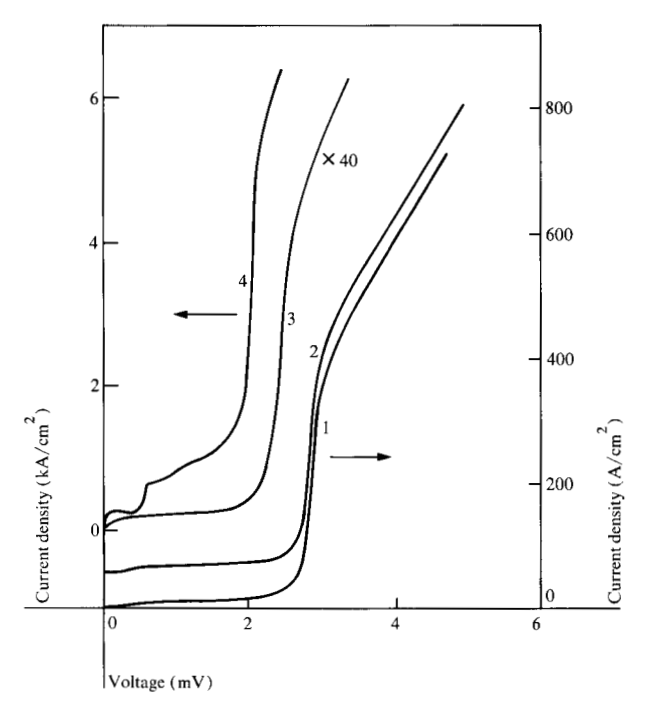


Figure 9 Single-particle-tunneling current as a function of voltage across the junction. Curves 1 and 2 (right-hand axis) were obtained from junctions formed on 13 and 22 at% In alloys, respectively (nominal process); samples mounted on Pb-coated rf electrode. Curve 3 is displaced upward for clarity. Curves 3 and 4 (left-hand axis) were obtained from junctions prepared using a similar oxidation procedure, except that Curve 4 is for a junction formed on an In-coated rf electrode. For Curve 3, the measured values of current density have been scaled up by a factor of 40 before plotting.

by suitably controlling the oxidation kinetics, it is possible to grow an rf oxide consisting entirely of this epitaxial In₂O₂. Alteration of the surface of that oxide by backscattering can be avoided by using an In-coated rf electrode or by choosing rf-oxidation conditions for which backscattering is negligible. Thus an oxide consisting entirely of In₀O₀ can be obtained. Such an oxide would be attractive for use as a tunnel barrier for Josephson devices if suitably low current density values could also be obtained. This single-phase oxide should exhibit improved chemical stability by comparison with the mixed PbO-In₂O₂ presently used for the tunnel barrier, due to the much lower free energy of formation of the In₂O₂. It should also be more reproducible, since the composition and structure of the mixed oxide are sensitive to variations in alloy composition and oxidation conditions. In addition, the epitaxial In₂O₃ is much simpler than the mixed oxide, a situation that may allow tunnel junctions to be modeled in terms of the physical properties of the oxide and the electrodes.

Acknowledgments

We thank R. W. Johnson and R. A. Pollak for permission to publish portions of the XPS studies done jointly with them. We also enjoyed helpful discussions with I. Ames, J. H. Greiner, and J. H. Magerlein regarding this work and the manuscript. Lastly, we thank R. A. Drake, A. Ginzberg, and W. K. Schug for their invaluable technical contributions.

References and notes

- 1. J. H. Greiner, J. Appl. Phys. 42, 5151 (1971).
- J. H. Greiner, S. Basavaiah, and I. Ames, J. Vac. Sci. Technol. 11, 81 (1974).
- 3. R. H. Havemann, C. A. Hamilton, and Richard E. Harris, J. Vac. Sci. Technol. 15, 392 (1978).
- 4. A. F. Hebard and R. M. Eick, J. Appl. Phys. 49, 338 (1978).
- 5. J. H. Greiner et al., IBM J. Res. Develop. 24 (1980, this issue).
- 6. S. K. Lahiri, J. Vac. Sci. Technol. 13, 148 (1976).
- S. K. Lahiri and S. Basavaiah, J. Appl. Phys. 49, 2880 (1978).
- N. J. Chou, S. K. Lahiri, R. Hammer, and K. L. Komarek, J. Chem. Phys. 63, 2758 (1975).
- J. M. Eldridge, D. W. Dong, and K. L. Komarek, J. Electron. Mater. 4, 1191 (1975).
- G. B. Donaldson and H. Faghihi-Nejad, in Proceedings on Future Trends in Superconductive Electronics, AIP Conf. Proc. No. 44, 407 (1978).
- John M. Baker, R. W. Johnson, and R. A. Pollak, J. Vac. Sci. Technol. 16, 1534 (1979).
- J. H. Greiner and S. Basavaiah, IBM Thomas J. Watson Research Center, Yorktown Heights, NY, private communication.
- 13. J. H. Greiner, J. Appl. Phys. 45, 32 (1974).
- 14. The PbInAu films are a two-phase alloy of a Pb(In) solid solution with an AuIn₂ precipitate phase [6]. These precipitates form below the surface; thus, during oxidation only the Pb-In solid solution phase is involved. Therefore, all compositions are cited in at% in the Pb-In phase of the alloy.
- D. R. Campbell, K. N. Tu, and R. E. Robinson, Acta Met. 24, 609 (1976).
- H. R. Koenig and L. I. Maissel, IBM J. Res. Develop. 14, 168 (1970).

- 17. A. T. Fromhold, Jr. (formerly with IBM; now with Dept. of Physics, Auburn University, Auburn, AL) and John M. Baker, unpublished results.
- 18. John M. Baker, unpublished results.
- 19. Frank L. McCrackin, *Technical Note 479*, National Bureau of Standards, Washington, DC, 1969.
- C. S. Fadley, in *Progress in Solid State Chemistry*, Vol. 11, part 3, J. McCaldin and G. Somorjai, Eds., Pergamon Press, Elmsford, NY, 1976, p. 265.
- A. J. Warnecke, R. M. Patt, and C. Johnson, Jr., in Proceedings of INTERFACE '77, Microelectronics Seminar, Kodak Pub. No. G-48, Rochester, NY, 1977, p. 145.
- Handbook of Chemistry and Physics, 49th Edition, R. C. Weast, Ed., Chemical Rubber Co., Cleveland, 1969.
- J. W. Matthews, C. J. Kircher, and R. E. Drake, *Thin Solid Films* 47, 95 (1977).
- J. W. Matthews, C. J. Kircher, and R. E. Drake, *Thin Solid Films* 42, 69 (1977).
- 25. S. K. Lahiri, Thin Solid Films 28, 279 (1975).
- J. L. Vossen, J. J. O'Neill, Jr., K. M. Finlayson, and L. J. Royer, RCA Rev. 31, 293 (1970).
- 27. J. H. Greiner, IBM Thomas J. Watson Research Center, Yorktown Heights, NY, private communication.
- 28. J. M. Eldridge, Y. J. Van der Meulen, and D. W. Dong, *Thin Solid Films* 12, 447 (1972).
- 29. H. K. Müller, Phys. Status Solidi 27, 723 (1968).
- 30. J. H. Magerlein, IBM Thomas J. Watson Research Center, Yorktown Heights, NY, private communication.
- 31. The lower energy gap (\approx 2.45 meV) observed for the junction prepared on the Pb-coated electrode is due to the lower $T_{\rm c}$ of the Pb-Au compared with the Pb-Bi alloy. The lower energy gap and higher current levels below the energy gap observed for the junctions prepared on the In-coated electrode by comparison with those prepared on the Pb-coated electrode are probably caused by self-heating of the junctions due to the high current densities required for the measurements.
- 32. T. R. Gheewala, *IBM J. Res. Develop.* 24, (1980, this issue).

Received April 20, 1979; revised July 27, 1979

John M. Baker and C. J. Kircher are located at the IBM Thomas J. Watson Research Center, Yorktown Heights, New York 10598. J. W. Matthews is deceased.